

# Modelling of an Explosion of an Improvised Explosive Device a Vehicle

Turza Jozef\*, Eliáš Jozef, Kopiláková Beáta, Rakúsová Danka

Faculty of Special Technology, Trenčín University of A. Dubček in Trenčín

\*Corresponding author: [jozef.turza@tnuni.sk](mailto:jozef.turza@tnuni.sk)

Received September 05, 2014; Revised September 15, 2014; Accepted October 09, 2014

**Abstract** An aim of the paper is to define behaviour of a combat vehicle based on an analysis of its movement from a point of a maximum vertical movement, acceleration and forces through development of a mathematical model of a vehicle during an operation of the vehicle in critical situations of a modern battlefield.

**Keywords:** *combat vehicle, explosives, an explosion, a system, mathematical model, a torque bar, a rocker, a damper, spring and rubber buffer, a vehicle hull*

**Cite This Article:** Turza Jozef, Eliáš Jozef, Kopiláková Beáta, and Rakúsová Danka, "Modelling of an Explosion of an Improvised Explosive Device a Vehicle." *American Journal of Mechanical Engineering*, vol. 2, no. 7 (2014): 209-215. doi: 10.12691/ajme-2-7-8.

## 1. Introduction

In deployment of a mechanized infantry an explosion of a charge under a vehicle may appear. The paper is aiming to make an analysis based on a developed mathematical model, what influence will it have on a vehicle's dynamics. In the paper there is a simplified mathematical model of behaviour of the vehicle. The model can determine what acceleration (hence power) influence a vehicle and what large vertical movements may occur. An issue of a vertical movement of a vehicle after an explosion of a charge [1,7] and in running over a bump is rather complicated; therefore some simplifications have been applied for the first analysis.

## 2. Description of Dynamics of Vehicle Movement in Explosion under a Vehicle

The BMP-2 combat vehicle has been taken for description of dynamics of a vertical movement of the vehicle, depicted with main parts needed for description of its dynamic features in the Figure 1. The traverse wheels with rockers and torque bars are important for a description, where a torque bar is a spring element for a vertical movement [1,2,3,6].

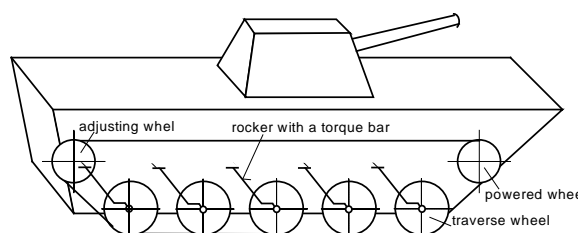


Figure 1. A view on a BMP-2 combat vehicle

An explosion of a charge under a vehicle is supposed in a lower part of a hull places under the gravity center of the vehicle.

As an issue of a movement of the vehicle is rather difficult, the following assumptions have been assumed for modelling [5,7]:

- an explosion will occur in the middle of the vehicle under its gravity center,
- the gravity center of the vehicle is situated symmetrically in a longitudinal as well as in a transverse direction,
- we consider no longitudinal, nor transverse vibration of the vehicle, we take only vertical movement of the vehicle into consideration,
- pressure during explosion is regularly distributed on a whole lower surface of the vehicle,
- distribution of forces is regular for all loaded wheels,
- a factor of dumpers absorption is considered as different for an engaging and disengaging of a dumper,
- dumpers are constantly connected with contact points,
- terrain under vehicle is considered flat, clearance of a vehicle is the same,
- vertical movement of the vehicle downwards is limited proportionally for four rockers through lamellar and for four rockers through rubber buffers.

### 2.1. The Vehicle as a Whole

Mathematical description of particular important parts of the vehicle is defined in a subsequent text. Particular important elements and groups needed for description of behaviour of the vehicle are described separately with certain simplification. There are independent units, as a hull of the vehicle, rockers with torque bars, dampers, and spring and rubber buffers of the vehicle. A separate chapter is a description of a force action from an explosion of an improvised charge on a vehicle bottom.

### 2.2. Vehicle Hull

With respect to the assumptions we are taking into consideration the forces are acting symmetrically only in a cross and longitudinal sections. The action of forces acting on the vehicle hull in a cross and longitudinal sections are illustrated in the Figure 2. There are forces from placing a torque bar  $F_A$ , from the weight of the vehicle  $G_v$ , a force from a vehicle acceleration  $F_{mv}$ , forces from dampers  $F_{il}$  from the first and the sixth pair of wheels, forces from a spring buffer  $F_{pr1}$  in the first and the sixth pair of wheels, forces from a spring buffer  $F_{pr2}$  in the second and the fifth pair of wheels having the number of rockers with wheels  $n_k=12$ .

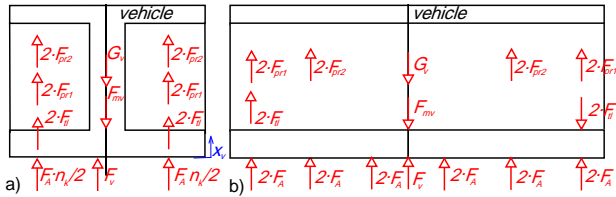


Figure 2 Action of forces on a vehicle hull; a) a cross section, b) a longitudinal section

From a balance of forces in a vertical direction the following relation applies.

$$G_v + F_{mv} - F_v - F_{il} \cdot 3 / n_k - F_A \cdot n_k - F_{pr1} \cdot 3 / n_k - F_{pr2} \cdot 3 / n_k = 0. \tag{1}$$

Gravitational force of the vehicle having an  $m_v$  weight is defined as

$$G_v = m_v \cdot g \tag{2}$$

and an accelerating force

$$F_{mv} = m_v \cdot \ddot{x}_v \tag{3}$$

The other forces and relations will be defined in the following text.

### 2.3. A Rocker with a Traverse Wheel and a Torque Bar

We suppose that a road has a flat surface. Kinematics of a movement and main parameters of a traverse wheel rocker with a torque bar is illustrated in Figure 3. We can simplify it for purposes of a dynamic analysis with a certain approximation as in Figure 4. An action of forces on a rocker in a vertical plane is illustrated in Figure 5. Let us simplify and choose a simulated rocker that the forces of a dumper, the forces of a spring and rubber buffer having a size with  $4/n_k$  ratio, are acting.

Then in a vertical plane there are acting forces on a simulated rocker as by Figure 5. Particularly there are defined the  $M_t$  momentum of a torque bar and a  $M_r$  momentum from a rotation of a rocker. An  $F_c$  force from a road at  $a_1$  distance implies an additional bending moment on a rocker and therefore a deformation as well. With regard to a massiveness of a rocker we are not taking its deformation into consideration for our purposes. We do not consider any vertical roughness of a road. The description is made for a group of a simulated rocker of a traverse Wheel with a torque bar. Through an implementation of a course of a vertical movement due to

a road roughness, a dynamic behaviour of a driving vehicle could be determined.

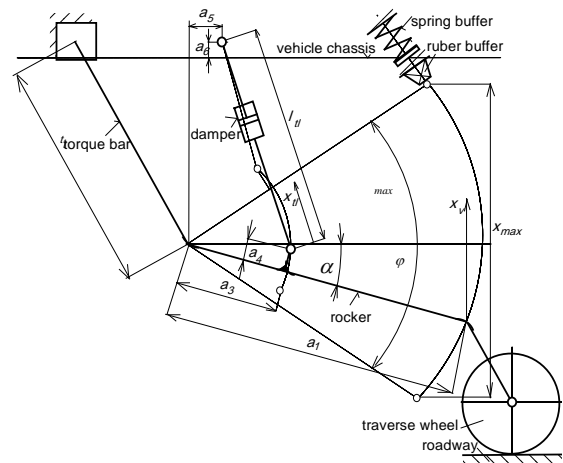


Figure 3. Kinematics of a movement of a rocker, a damper, a rubber and a spring buffer

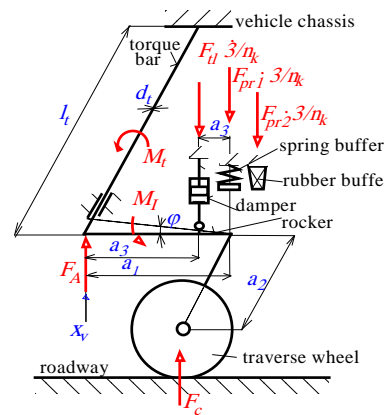


Figure 4. Forces acting on a rocker in an explosion of a charge in a simplified way

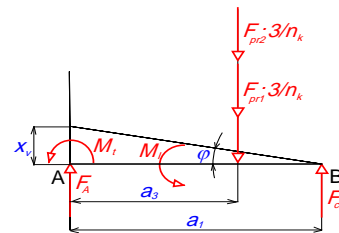


Figure 5. Forces acting on a simulated rocker with a wheel in a vertical plane

In Figure 5 there are illustrated all stresses applied to the rocker in a vertical plane. The principle of a movement of a rocker, damper, a rubber and a spring buffer is delineated there. The movement will be explored only on the only one rocker. The number of rockers is  $n=12$ , number of spring buffers is four and number of rubber buffers is four. The weight of a vehicle per a rocker is reduced in  $1/n_k$  ratio, therefore the number of buffers is also considered in 1:4 ratio. An uplift of a rocker (vehicle) will be considered approximately

$$x_v = a_1 \cdot \sin \phi \tag{4}$$

The  $M_t$  torque of a torque bar, having an  $l_t$  length of a torque bar, the  $G_t$  modulus of elasticity in shear and a  $J_t$  polar square moment of a torque bar cross-section having a  $d_t$  diameter causes twisting of a rocker by an angle

$$\phi = \frac{M_t \cdot l_t}{G_t \cdot J_t} \Rightarrow M_t = \frac{G_t \cdot J_t}{l_t} \cdot \phi = k_t \cdot \phi \quad (5)$$

where a polar square moment of a torque bar cross-section is defined from a relation

$$J_t = \frac{\pi \cdot d_t^4}{32} \quad (6)$$

Stiffness of a rocker torque bar is defined using an equation (5)

$$k_t = \frac{G_t \cdot J_t}{l_t} = \frac{G_t \cdot \pi \cdot d_t^4}{32 \cdot l_t} \quad (7)$$

There are applied similar relations between a twisting  $\phi$  and a shift of a vehicle body in large and small deformations

$$\begin{aligned} x_v &= a_1 \cdot \sin \phi \approx a_1 \cdot \phi \\ \dot{x}_v &= a_1 \cdot \cos \phi \cdot \dot{\phi} \approx a_1 \cdot \dot{\phi} \\ \ddot{x}_v &= a_1 \cdot (-\sin \phi \cdot \ddot{\phi} + \dot{\phi}^2) \approx a_1 \cdot \ddot{\phi} \end{aligned} \quad (8)$$

We suppose balanced loading of all rockers of traverse wheels with torque bars. A reduced  $I_r$  moment of inertia for a rotational movement of a rocker with a Wheel is calculated based on a relation

$$M_I = I_r \cdot \ddot{\phi} \quad (9)$$

where  $I_r$  is a mass moment of inertia of a rocker arm of a traverse wheel and a torque bar. For a vertical movement of an A point (Figure 5) the equation of a balance in a vertical direction is applied

$$F_A + F_c - \frac{3}{n_k} \cdot F_{tl} - \frac{3}{n_k} \cdot F_{pr1} - \frac{3}{n_k} \cdot F_{pr2} = 0 \quad (10)$$

a torque equation to A point

$$\begin{aligned} F_c \cdot a_1 + M_t + M_I - \frac{3}{n_k} \cdot F_{tl} \cdot a_3 \\ - \frac{3}{n_k} \cdot F_{pr1} \cdot a_1 - \frac{3}{n_k} \cdot F_{pr2} \cdot a_1 = 0 \end{aligned} \quad (11)$$

respectively to B point

$$F_A \cdot a_1 - \frac{G_v}{n_k} \cdot a_1 - M_t - M_I - \frac{3}{n_k} \cdot F_{tl} \cdot (a_1 - a_3) = 0 \quad (12)$$

The buffer forces  $F_{pr1}$  and  $F_{pr2}$  start acting only after having finished an  $x_{max}$  uplift (Figure 3). A mass moment of inertia for  $I_{vr}$  rocker is computed based on a relation

$$I_{vr} = \frac{1}{32} \cdot \rho \cdot \pi \cdot d_t^4 \cdot l_t + m_{vah} \cdot r_{vah}^2 \quad (13)$$

After having substituted real values for simulation we receive

$$\begin{aligned} I_{vr} &= 7850 \cdot \pi \cdot 0.038^4 \cdot 2 / 32 + 25 \cdot 0.15^2, \\ I_{vr} &= 0.5657 \text{ kg} \cdot \text{m}^2. \end{aligned} \quad (14)$$

## 2.4. Damper

It is a double action hydraulic damper, the manufacturer states from testing with 40 double lifts per minute its

mean power 3.25 kN in piston rod disengagement and 13 kN in piston rod engagement at  $h_r=0.1$  m uplift. As a speed of a piston rod uplift in testing is the same in engagement and disengagement, time of uplift is

$$t_z = 60 / (2 \cdot 40) = 0.75 \text{ s} \quad (15)$$

and a speed of uplift is

$$v_t = h_t / t_t = 0.1 / 0.75 = 0.13333 \text{ m/s}. \quad (16)$$

a coefficient of a damping the piston rod down in disengaging is

$$f_{tl2} = F_2 / h_t = 3250 / 0.1 = 32.5 \text{ kN/m} \quad (17)$$

and a coefficient of a damping the piston rod down in engaging is

$$f_{tl1} = F_1 / h_t = 13000 / 0.1 = 130 \text{ kN/m}. \quad (18)$$

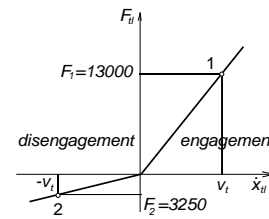


Figure 6. Linear characteristics of a damper for engagement and disengagement of a piston rod

A force of a damper can be expressed by an equation

$$F_{tl} = f_{tl1} \cdot \dot{x}_{tl} \cdot (\dot{x}_{tl} \geq 0) + f_{tl2} \cdot \dot{x}_{tl} \cdot (\dot{x}_{tl} < 0) \quad (19)$$

An uplift of a damper on a rocker will be approximately

$$x_{tl} = a_3 \cdot \sin \alpha = a_3 \cdot x_v / a_1 \quad (20)$$

## 2.5. Spring Buffer

A plate spring has been used in form of an Archimedean spiral in conformity with Figure 7. Basic dimensions for computation were: number of convolutions  $n_l=7$ , final angle of a spiral  $\varphi_{p1}=0.1$  rad,  $\varphi_{p2}=0.1833$  round, plate width  $h_l=92$  mm, plate thickness  $b_l=4$  mm, maximum compression  $x_{dm}=86.6$  mm, radius of a spiral origin  $r_l=12$  mm, radius of a spiral end  $r_2=44$  mm, modulus of elasticity of a plate material  $E_l=210$  GPa.

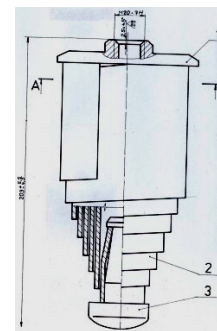


Figure 7. Construction of a plate buffer in a shape of an Archimedean spiral

A square moment of a cross-section

$$I_l = b_l \cdot h_l^3 / 12 = 0.004 \cdot 0.092^3 / 12 = 25.96 \times 10^{-8} \text{ m}^4. \quad (21)$$

Length of a spiral plate

$$s = r_2 \cdot [1 + \pi \cdot n - \phi_{p2} / 2] - r_1 \cdot [1 + \pi \cdot n - \phi_{p1} / 2],$$

$$s = 44 \cdot [1 + \pi \cdot 7 - 1.83333 / 2] - 12 \cdot [1 + \pi \cdot 7 - 0.1 / 2] \quad (22)$$

$$= 0.7347 \text{ m.}$$

Length of a plate of an Archimedean spiral

$$L = \sqrt{s^2 + x_{dm}^2} = \sqrt{0.7347^2 + 0.0866^2} = 0.74 \text{ m.} \quad (23)$$

Stiffness of a plate spring

$$k_{pr1} = 3 \cdot E \cdot I_l / L^3 \quad (24)$$

$$= 3 \cdot 2.1 \cdot 10^{11} \cdot 25.9563 \cdot 10^{-8} / 0.7398^3 = 4.08 \times 10^5 \text{ N / m.}$$

After having finished an uplift of a spring, stiffness of a buffer will be

$$k_{dor} = E_l \cdot b \cdot L / h = 2.1 \cdot 10^{11} \cdot 0.004 \cdot 0.7398 / 0.923 \quad (25)$$

$$= 8.4 \times 10^8 \text{ N / m.}$$

Course of a spring force will be

$$F_{pr1} = k_{pr1} \cdot x_{pr1} \cdot ((x_v - x_{max}) \geq 0) \quad (26)$$

$$+ k_{dor} \cdot (x_v - x_{max}) \cdot ((x_v - x_{max} - x_{dm}) \geq 0)$$

in compression of a plate spring

$$x_{pr1} = x_v - x_{max} \cdot \quad (27)$$

Course of forces of a plate spiral spring and a fixed buffer is illustrated in the Figure 8.

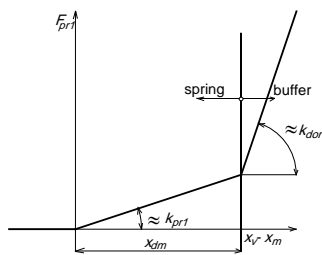


Figure 8. Course of forces of a plate spring buffer and a fixed buffer

## 2.6. Rubber Buffer

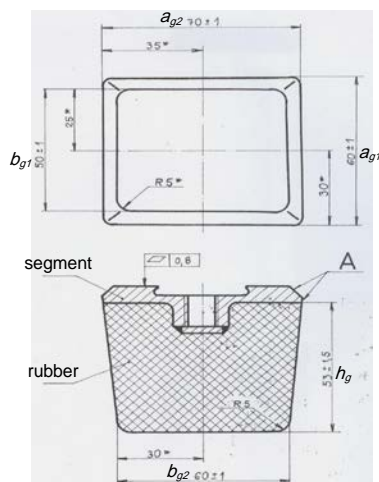


Figure 9. Construction of a rubber buffer

Construction of a rubber buffer is illustrated in the Figure 9. A rubber is vulcanically connected on a segment. A segment is firmly attached to a vehicle hull with a

bolted connection. The dimensions and data on a rubber in accordance with the manufacturer's data are  $a_{g1}=60 \text{ mm}$ ,  $a_{g2}=70 \text{ mm}$ ,  $b_{g1}=50 \text{ mm}$ ,  $b_{g2}=60 \text{ mm}$ ,  $h_g=53 \text{ mm}$ . A dynamic modulus of elasticity in pressure for a used rubber is considered to be  $E_g=10 \text{ MPa}$ .

Compression of a rubber buffer is computed through a relation

$$x_{pr2} = \frac{F_{pr2}}{E_g} \cdot \int_0^{h_g} \frac{dx}{\left( a_{g1} + \frac{a_{g2} - a_{g1}}{h_g} \cdot x \right) \cdot \left( b_{g1} + \frac{b_{g2} - b_{g1}}{h_g} \cdot x \right)} \quad (28)$$

$$= \frac{F_{pr2} \cdot h_g^2}{E_g \cdot (a_{g2} - a_{g1}) \cdot (b_{g2} - b_{g1})} \cdot \int_0^{h_g} \frac{dx}{(k_1 + x) \cdot (k_2 + x)},$$

Where  $k_1, k_2$  are auxiliary constants

$$k_1 = \frac{a_{g1} \cdot h_g}{a_{g2} - a_{g1}}, k_2 = \frac{b_{g1} \cdot h_g}{b_{g2} - b_{g1}} \quad (29)$$

Through an integration of an equation 28 and using constants from an equation 29 we receive

$$x_{pr2} = \frac{F_{pr2} \cdot h_g}{E_g \cdot (a_{g1} \cdot b_{g2} - a_{g2} \cdot b_{g1})} \cdot \ln \left| \frac{a_{g1} \cdot b_{g2}}{a_{g2} \cdot b_{g1}} \right| \quad (30)$$

From equation 30 after an adjustment a stiffness of a rubber buffer can be obtained in a following form

$$k_{pr2} = \frac{F_{pr2}}{x_{pr2}} = \frac{E_g \cdot (a_{g1} \cdot b_{g2} - a_{g2} \cdot b_{g1})}{h_g \cdot \ln \left| \frac{a_{g1} \cdot b_{g2}}{a_{g2} \cdot b_{g1}} \right|} \quad (31)$$

After having substituted the dimensions and parameters of a rubber buffer into an equation 31 we receive an intensity of stiffness

$$k_{pr2} = \frac{1 \cdot 10^7 \cdot (0.06 \cdot 0.06 - 0.07 \cdot 0.05)}{0.053 \cdot \ln \left| \frac{0.06 \cdot 0.06}{0.07 \cdot 0.05} \right|} \approx 700 \text{ kN / m.} \quad (32)$$

Relation for computation of a force of a rubber buffer will be

$$F_{pr2} = k_{pr2} \cdot x_{pr2} \quad (33)$$

Course of a force of a rubber buffer is drawn by an equation 33 in the Figure 10.

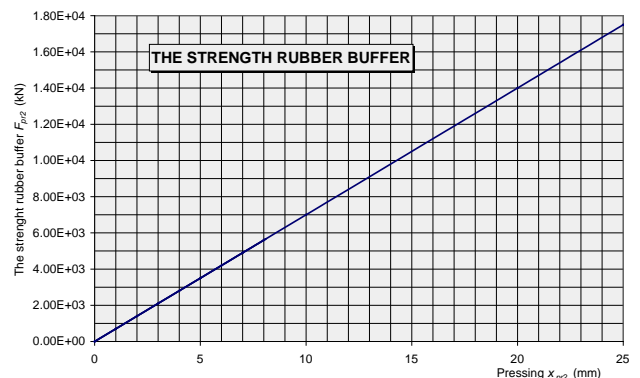


Figure 10. Course of a force of a rubber buffer

### 2.7. Forces from an Explosion on a Vehicle

An overpressure spreads on a front of a blast wave in an explosion of a charge in spherical surfaces. The time of a rise and a discharge of a blast wave are very short, in order up to 20 ms. Makovička was dealing with modelling of a course of a blast wave in more details [7] and he defined the most probable course. His model has been used in the next text for our case. A value of an overpressure on a front of a blast wave will be calculated through following relations. A reduced spacing distance from an  $R_p$  explosion epicenter will be calculated through a distance from an epicenter of an  $R$  charge explosion in m, a total equivalent mass of a charge  $C_w$  in  $m/kg^{1/3}$  from a relation

$$R_p = \frac{R}{C_w^{1/3}} = \frac{(x^2 + y^2 + R_0^2)^{1/2}}{C_w^{1/3}} \quad (34)$$

There is a different value of an overpressure (Figure 11) acting at each point P on a bottom of a vehicle having dimensions  $a_v$ ,  $b_v$  on an element of a surface  $dA=dx \cdot dy$  at  $R$  distance. This value will be calculated from a relation

$$R = \sqrt{x^2 + y^2 + R_0^2} \quad (35)$$

where  $R_0$  is a vertical distance of a lower surface of the vehicle from a road,  $x$ ,  $y$  are coordinates of the P point in a coordinate system  $x$ ,  $y$ .

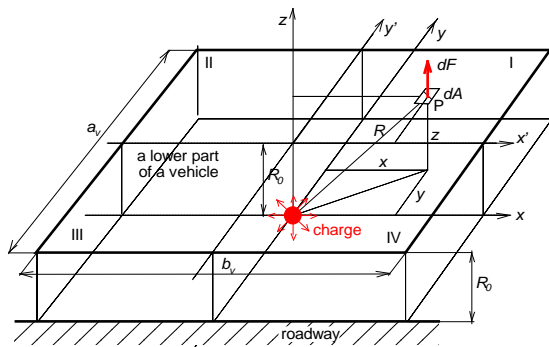


Figure 11. Exerting pressure explosion charges under the vehicle

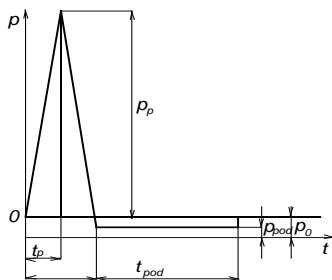


Figure 12. Values of a course of a maximum overpressure

A total equivalent mass of a charge in kg TNT (trinitrotoluene) is defined from a relation

$$C_w = C_N \cdot k_{NTp} \cdot k_E \cdot k_G \quad (36)$$

Where  $C_N$  is a weight of a used charge of an explosive in kg,  $k_{NTp}$  is a pressure TNT equivalent,  $k_E$  coefficient of a charge sealing,  $k_G$  coefficient of a geometry of a blast wave spreading in a space (for a detonation in a free space  $k_G=1$ , on a terrain surface  $k_G=2$ ),  $k_B$  is a ballistic ratio

(ratio of a case weight in kg/ to weight of explosives in kg). A sealing coefficient is defined based on relation

$$k_E = 0.2 + 0.8 \cdot (1 + k_B) \quad (37)$$

A size of an overpressure in MPa on a front of a blast wave for a ground explosion in MPa at a ground explosion in external environment for  $R_p \leq 1$  (in our case the term is applied

$$p_p = \frac{1.07}{R_p^3} - 0.1 = \frac{1.07 \cdot C_w}{R^3} = \frac{1.07 \cdot C_w}{(x^2 + y^2 + R_0^2)^{3/2}} - 0.1 \quad (38)$$

An overpressure in an overpressure phase of a blast wave in Mpa

$$p_{pod} = \frac{0.035}{R_p} = \frac{0.035 \cdot C_w^{1/3}}{(x^2 + y^2 + R_0^2)^{1/2}} \quad (39)$$

Duration of an overpressure wave in s

$$t_p = 1.6 \cdot 10^{-3} \cdot C_w^{1/6} \cdot R^{1/2} \quad (40)$$

Duration of an under pressure wave in s

$$t_{pod} = 1.6 \cdot 10^{-3} \cdot C_w^{1/3} \quad (41)$$

Course of an overpressure and an under pressure wave in time by previous relations is illustrated in figure, where  $p_0$  is a pressure of an environment. For different 4 values of a charge weight in kg of TNT a Figure 13 illustrates a maximum value of an overpressure for a vertical distance from a bottom surface of vehicle from a road  $R_0=0.5$  m.

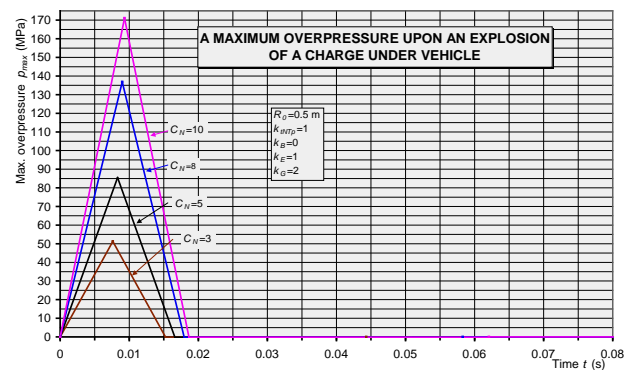


Figure 13. Course of a maximum overpressure on a blast wave head under a vehicle

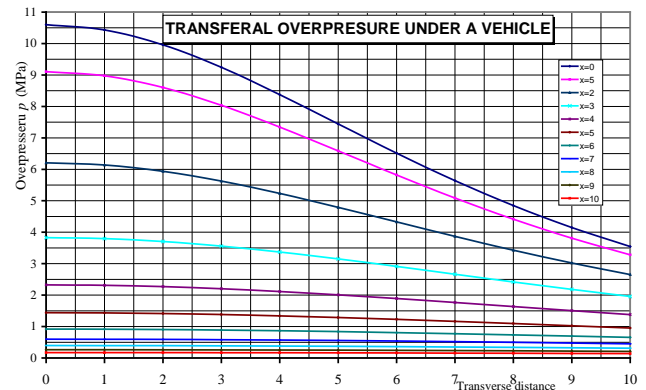


Figure 14. Course of maximum stresses in quadrant I for different sections in a cross direction  $x=(1 \div 10)$

In a selected I quadrant a bottom of a vehicle is divided through a grid into ten sections in a cross direction of a vehicle ( $x=1\div 10$ ) and also into ten sections in a longitudinal direction ( $y=1\div 10$ ).

Figure 14 illustrates a course of maximum overpressures in a cross-section in  $t_p$  time and the Figure 15 in a longitudinal direction.

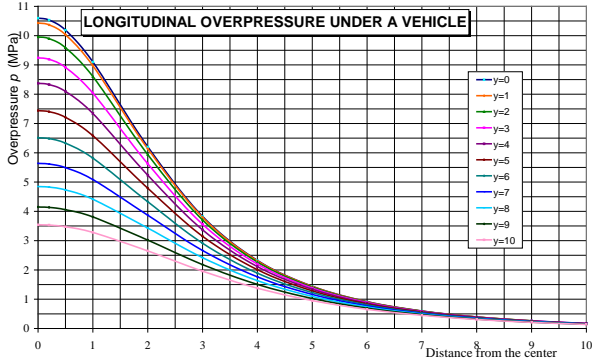


Figure 15. Course of maximum overpressures in the I. quadrant for different sections in a longitudinal section  $y=(1\div 10)$

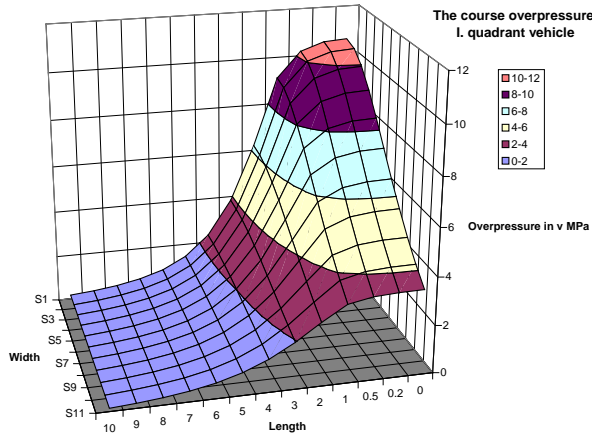


Figure 16. Spatial representation of a maximum value of a pressure in the I quadrant in a cross and longitudinal directions

Based on courses we can note, that if a blast wave leaves in a longitudinal direction, the value of a maximum pressure is lower than if it leaves under a vehicle in a cross direction. It relates a symmetric action of an overpressure on a bottom part of the vehicle, therefore a calculation can be done only for one quadrant, and for example the first one and a resulting force will be multiplied by 4 x. A value of an under pressure is very small, therefore it will be neglected for a next calculation of forces from a charge explosion. A size of maximum acting force acting on a bottom of a vehicle in  $t_p$  time in accordance with Figure 11 can be defined based on a relation

$$F_v = 4 \cdot 10^6 \cdot \int_0^{b_v/2} \int_0^{a_v/2} \left[ \frac{1.07 \cdot C_w}{(x^2 + y^2 + R_0^2)^{3/2}} - 0.1 \right] \cdot dx \cdot dy. \quad (42)$$

After integration and adaptations from the equation 42 we receive

$$F_v = 4 \cdot 10^6 \cdot \left( \begin{matrix} 1.07 \cdot C_w \cdot \frac{1}{R_0} \cdot \arctg \left( \frac{a_v \cdot b_v}{2 \cdot R_0 \cdot \sqrt{a_v^2 + b_v^2 + 4 \cdot R_0^2}} \right) \\ -0.1 \cdot \frac{a_v \cdot b_v}{4} \end{matrix} \right). \quad (43)$$

In case, we would considered, that under a whole surface of a vehicle there is acting a maximum overpressure, a value of a maximum force in  $t_p$  time would be

$$F_v^* = p_d \cdot a_v \cdot b_v. \quad (44)$$

A course of a force is acting on a bottom of a vehicle in  $t_p$  time only with a maximum value of  $F_v$  in time  $t_p/2$ , it means in a form of an isoscelent pulse (Figure 12, respectively for particular values by a Figure 13). With respect to small dimensions of a vehicle we do not consider any regressive blast wave.

For combat vehicles we need to consider mostly the mass of a used charge up to  $C_N=5$  kg TNT placed just about a terrain surface, where  $k_G=2$ .

### 3. Simulation Model

A simulation model has been made up in a computation model DYNAST based on above mentioned equations for a particular vehicle through impedance networks. A block simulation model is shown in the Figure 17. Stiffness of a torque bar with a rocker using equations 5 and 7 with a length of a torque bar  $l_t=1.93$  m, its modulus of elasticity in a material shear  $G_t=78.5$  GPa and a diameter  $d_t=38$  mm is

$$k_t = \frac{G_t \cdot \pi \cdot d_t^4}{32 \cdot l_t \cdot a_t^2} = \frac{78.5 \cdot 10^9 \cdot \pi \cdot 0.038^4}{32 \cdot 1.93 \cdot 0.325^2} \quad (45)$$

$$k_t = 78.828 \text{ kN / m.}$$

In balanced stable conditions a  $\phi_{st}$  deformation of rockers is defined using equations 8 and 11, equations 11 and 12 and further adjustment without taking forces of a damper and buffers into consideration as follows

$$\phi_{st} = \frac{32 \cdot m_v \cdot g \cdot l_t \cdot a_1}{n_k \cdot G_t \cdot \pi \cdot d_t^4} = \frac{32 \cdot 12.8 \cdot 10^3 \cdot 9.81 \cdot 1.93 \cdot 0.3}{12 \cdot 78.5 \cdot 10^9 \cdot \pi \cdot 0.038^4} \quad (46)$$

$$= 0.377 \text{ rad.}$$

with a corresponding angle  $\phi_{st}=2.202^\circ$ , respectively a static compression in accordance with equation 8

$$x_{vst} = a_1 \cdot \phi_{st} = 300 \cdot 0.377 = 113.1 \text{ mm.} \quad (47)$$

This value will be an initial condition for a further solution in a simulation. The previous values were calculated for a length of a torque bar  $l_t=1.93$  m, diameter of a torque bar  $d_t=38$  mm, weight of a vehicle  $m_v=12800$  kg, gravity acceleration  $g=9.81$  m/s<sup>2</sup>.

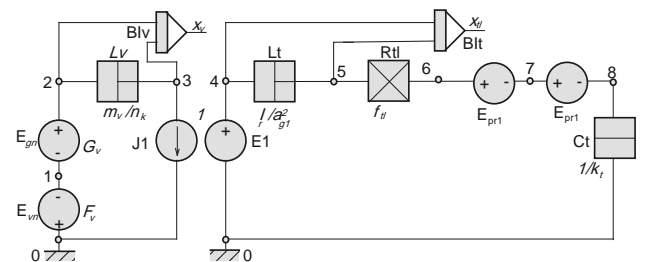


Figure 17. A block simulation model for an explosion of a charge under a vehicle

Aiming to form a block simulation modul there were used an Rtl movement resistance observing a damping

feature of a damper, an  $L_t$  acceleration resistance describing a mass moment of inertia of a rocket and attached masses,  $C_t$  capability of a torque bar observing stiffness of a torque bar, a  $E_{pr1}$  source respecting a feature of a spring buffer, a  $E_{pr2}$  observes a feature of a rubber buffer,  $L_v$  an acceleration resistance observing a mass of a vehicle, the  $E_{pm}$  source observes a mass of a vehicle,  $E_v$  source of force from explosion,  $J_1$  and  $E_1$  represent a transformer of a vehicle movement and a rocker movement,  $B_{lv}$  and  $B_{lt}$  are integrating blocks to define uplifts of a vehicle  $x_v$  and uplift at the end of a rocker  $x_r$ . Theory in more details is mentioned in [8].

## 4. Results of a Simulation

Some results of a simulation of the explosion under a vehicle with a charge of size  $C_N=5$  kg TNT in accordance with data from a previous text are drawn in the Figure 18.

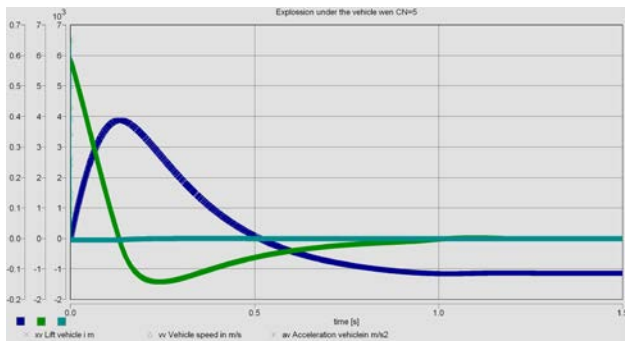


Figure 18. Results of simulation of a charge explosion under a vehicle

A course  $x_v$  of a vehicle uplift is drawn in the Figure 18, having a  $v_v$  speed of the uplift and an  $a_v$  acceleration in a vertical direction during an explosion of a charge under a centre of a vehicle. From courses it can be seen that a maximum uplift of a vehicle is 388 mm at 10.8 ms, a minimum uplift -115 mm, becoming stabilized after 1.5 s. Speed of uplift is maximum at 5.873 m/s in time 16.5 ms and minimum -1.419 m/s in time 1.5 s. A maximum value of acceleration is 6542 m/s<sup>2</sup> in time of 1 ms and minimum -46.92 m/s<sup>2</sup> in time of 56.5 ms. A value of a maximum acceleration for a charge being considered is significant and it has a great influence on a vehicle crew. The values would be lesser if also deformation and damping features of the vehicle hull would be taken into consideration. At computed accelerations it would be difficult to design the seats of a crew that would eliminate an effect of acceleration.

Size of a maximum force at explosion would be  $F_{vm}=7.69$  MN of a saw-tooth pulse lasting  $t_{max}=1.66$  ms.

From values of courses in the Figure 18 we can note that kinematics, used stiffness of rockers and dampers of the vehicle are designed very well and they provide for a

strong aperiodic course without additional vibration after a vehicle incidence.

## 5. Conclusions

A generated simplified mathematical model and results of a simulation have shown that a construction of a chassis is very well designed.

It has been proved that action by force from an explosion of a charge of a size of  $C_N=5$  kg TNT is significant, mainly a value of an acceleration of a vertical movement of a vehicle.

Based on verification by a created program we are presenting its improvements also for an explosion of a charge aside from a vehicle centre.

## Acknowledgement

This publication was created in the frame of the project "Alexander Dubček University of Trenčín wants to offer high-quality and modern education", ITMS code 26110230099, based on the Operational Programme Education and funded from the European Social Fund.

## References

- [1] Eliaš, J. 2013: Zvýšenie bezpečnosti členov roja bojového vozidla pri jazde v ťažkých terénnych podmienkach moderného bojiska. (Increase the safety of members combat vehicle group when driving in off road conditions of the modern battlefield). In: Zborník prednášok zo 14. medzinárodnej vedeckej konferencie Transfér 2013, 17-18. október 2013. Trenčín, FŠT TnU AD 2013.
- [2] Eliaš, J., 2002. Špeciálna mobilná technika na pásových podvozkoch: Charakteristiky, Technické údaje a popis. (Special mobile equipment tracked: Features, Specifications and description.) Issue 1. Trenčín: TnU, 2002.
- [3] Ferencey, V., Dropa, P. 2005. Mechanika pohybu pásovej mobilnej techniky. (Mechanics of movement band mobile technology). Trenčín: TnU, 2005.
- [4] Makovička, D, Makovička, D. ml.: Design of bulding structure loaded by explosion shock wave. Available. [http://www.makovicka.cz/publikace/2009\\_po\\_cz.pdf](http://www.makovicka.cz/publikace/2009_po_cz.pdf).
- [5] Skřehot, P. 2009. Prevence nehod a havárií. Časopis výzkumu a aplikací v profesionální bezpečnosti. (Prevention of incidents and accidents. Magazine research and applications in the professional security). 2009, roč. 2, č. 4.
- [6] Sloboda, A., Ferencey, V., Hlavňa, V., Tkáč, Z. 2008: Konštrukcia kolesových a pásových vozidiel. (The design of wheeled and tracked vehicles). Viena, Košice 2008.
- [7] Turza, J., Eliaš, J. 2013: (Analysis of dymamic features of mine trap effects on a crew of a combat vehicle). In: Zborník prednášok zo 14. medzinárodnej vedeckej konferencie Transfér 2013, 17-18. október 2013. Trenčín, FŠT TnU AD 2013.
- [8] Turza, J., Tkáč, Z., Vanc, M., Bucha, J., Rybičková, L., Čelko, P., Kleinedler, P. 2009. Axiálne piestové hydrostatické prevodovníky: Teória a výpočet. (Axial piston hydrostatic pump and motor. Theory and calculation.). Issue 1 - Trenčín: Trenčianska univerzita Alexandra Dubčeka, 2009.